EUV IMAGING SPECTROMETER
Hinode

EIS SOFTWARE NOTE No. 10

Version 1 6 January 2010

CCD Dark Current and Bias

Paul Bryans
Naval Research Laboratory
Code 7670
Washington, DC 20375, USA

pbryans@ssd5.nrl.navy.mil

1 Overview

The following document provides an overview of issues related to the CCD dark current and CCD bias (or pedestal) that are present on the readout from the EIS detectors. We discuss the procedure used by `eis_prep` to remove the dark current, and highlight the resulting issues of which the user should be aware.

The dark current is seen to vary both in time and with position on the detector; the distribution of the dark current about its average has increased over time, and there is variation in the dark current level with wavelength and slit position. However, `eis_prep` treats the dark current value as constant over the detector, introducing error to the spectrum. The purpose of this document is to evaluate the effects of treating the dark current as a constant, and quantify their impact on data analysis.

2 Bias and Dark Current Subtraction

The raw data spectra are found to sit on a background of around 500 DN that arises principally from the CCD bias (or pedestal), and secondly from the CCD dark current. The default method of subtracting the bias and dark current employed by `eis_prep` is to determine the background level from the science data themself. The exact method of estimating this value is dependent on whether the observation used wavelength windows or a full CCD spectrum; further details are given in Section **??**. In either case, once determined, the background level is assumed to be constant over the data window. This constant background value is subtracted from the spectra by `eis_prep`.

One failing of subtracting such a constant bias and dark current is that it can result in pixels with negative DN values. The default mode for `eis_prep` sets pixels with zero or negative DN values to be missing data. This is because it is not possible to assign a photon noise error to the data points. However, particularly for full CCD spectra observing regions of low emission, the number of pixels with negative DN values can be significant. By setting the `/retain` keyword in `eis_prep`, pixels with zero or negative DN values will not be flagged as missing. The errors for these pixels will be set to the dark current error estimate.

3 Test Data

For the tests performed here, we have used the data from dark frame calibration exposures. These exposures are run periodically with the shutter closed for the purpose of identifying warm and hot pixels (see Section **??**). With the warm and hot pixels removed, these exposures result in a measure of the bias and dark current.

The full CCD height measures 1024 rows while the slit measures 512 CCD rows. The middle 512 rows of the CCDs were used at the beginning of the mission until January 2008 when the change was made to read-out the full CCD height. The dark frame exposures are for the middle 512 rows until 18th January 2008. From the 19th January 2008 onwards the dark frame exposures are for the full CCD height (split into rows 1–512 and rows 512-1023 rows; row 0 is not read out). The bottom rows are read using EIS study `regcal071` and the top rows are read using EIS study `regcal072`.

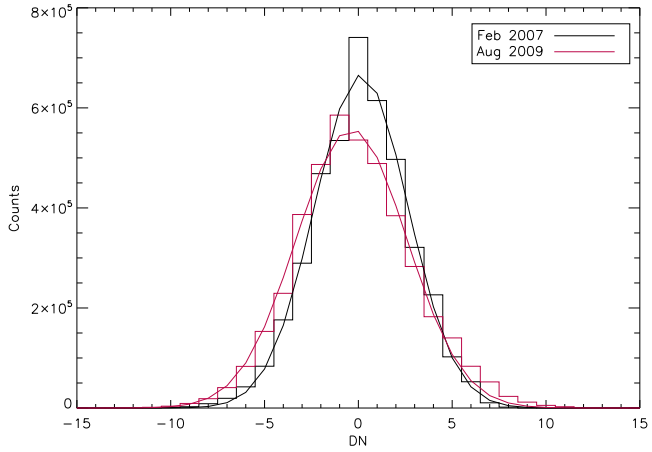

Figure 1: Histograms showing the spread of the dark current values over the detector, with Gaussian fits superimposed on the data. The black curve shows dark current values from the 21 February 2007 exposure and the red curve shows dark current values from the 15 August 2009 exposure.

Dark frame exposures are generally taken once per week. Here, we have sampled both top and bottom pixel maps in 6 month intervals from February 2007 to August 2009. Data are read out in four channels for every exposure, with each detector split into two wavelength windows. The pedestal is not constant over the four read-out channels. We have applied `eis_prep` using the `/noabs` keyword to each of the files listed above. This results in the removal of warm and hot pixels, and the subtraction of a constant bias plus dark current estimate. The value of this background level is estimated separately for each read-out channel.

4 Temporal Variations

There has been some degradation in the constancy of the dark current over the *Hinode* mission thus far. Figure 1 shows histograms of the intensity from the dark frame exposures for the datasets on 2007 Feb 21 and 2009 Aug 15 (the earliest and latest of the files sampled here). The figure shows a Gaussian distribution fitted to the dark current intensities. The standard deviation of these fits is 2.5 and 3.0 for the 2007 Feb 21 and 2009 Aug 15 exposures, respectively.

In addition to the increase in dark current standard deviation, the wavelength and spatial variations have also become more pronounced over the mission's lifetime. This is expanded upon in the following sections.

5 Wavelength Variations

Figure 2 shows the dark exposure results, for the short wavelength and long wavelength detectors, as a function of wavelength after averaging over the 512 spatial pixels of the slit. We show only the bottom CCD pixels; a similar variation with wavelength is seen in the top CCD pixels.

There is a variation in the dark current value with wavelength in all four detector sections. The

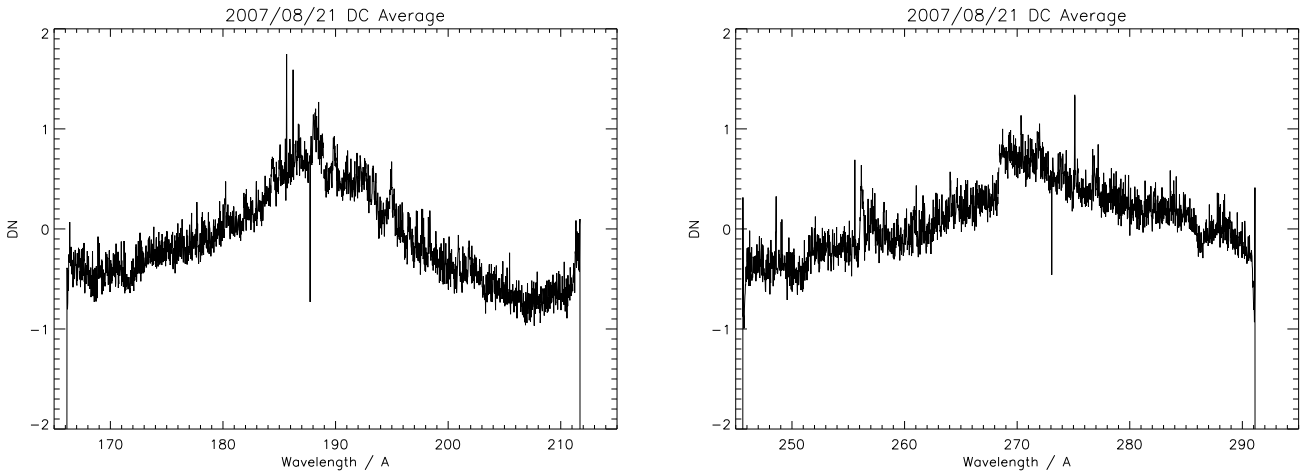

Figure 2: The variation of the dark current with wavelength, averaged over the slit height, for the 21 August 2007 dark frame exposure. The left panel shows the short wavelength detector and the right shows the long wavelength detector.

short wavelength quadrants of the short and long wavelength detectors show an increasing trend of the dark current with wavelength, while the long wavelength quadrants of the short and long wavelength detectors show an decreasing trend of the dark current with wavelength.

There are also areas of the detector showing small intensity peaks. We find that these peaks in intensity correspond to the wavelengths of the strongest emission lines detected by EIS. It would appear that the CCD pixels are displaying a residual 'burn in' at the locations of the strongest emission lines. However, if this were the case, one would expect these peaks in intensity to increase with time while in fact they are not evident in all dark frame exposures. Figure 3 shows examples of the dark current in the region of the He II 256 Å and Fe XII 195 Å lines, each for 3 dark current exposures. Only the 21 August 2007 exposure shows a peak at the wavelength of the He II line. The 23 February 2008 exposure shows a peak at the wavelength of the Fe XII line, while the 21 August 2007 exposure shows a peak that is offset by 1–2 Å, and the 21 February 2007 exposure shows no indication of increased intensity at this wavelength. It may be the case that some residual light is making its way onto the detector even while the shutter is closed in certain instances. Further work is required to determine if this is so.

6 Spatial Variations

Dark exposure maps are returned in arrays of 512 spatial pixels (along the slit) and 1024 wavelength pixels. Figure 4 shows the variation of the dark current with slit position after averaging over the wavelength window. The black curve is from a dark frame exposure near the beginning of the mission (21 February 2007) and the red curve is from a dark frame exposure on 15 August 2009. No significant variation was found between the four wavelength windows; we show only the long wavelength channel of the long wavelength detector in Figure 4 as representative of all channels.

There is an overall increasing trend of the dark current with slit height for both the top and bottom pixels. Furthermore, there is a sharp rise in the dark current over the first ∼30 pixels. That this same rise is evident in both the top and bottom pixels suggests it is due to the CCD bias or

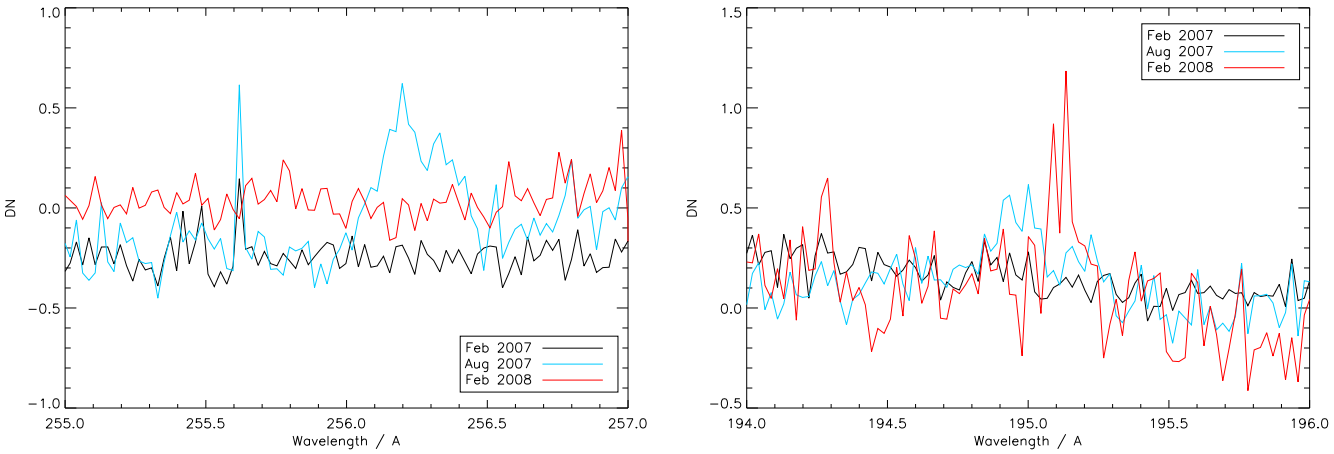

Figure 3: Dark current values at the wavelengths of the strong emission lines He II 256 Å (left panel) and Fe XII 195 Å (right panel). The black curve shows data from a dark frame exposure on 21 February 2007, the blue curve shows data from 21 August 2007, and the red curve shows data from 23 February 2008.

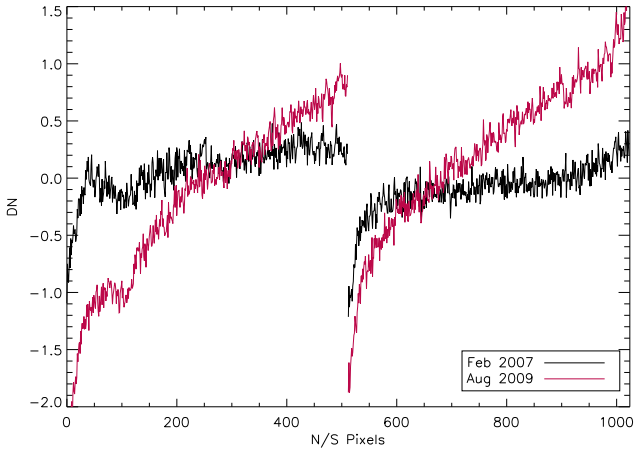

Figure 4: The variation of the dark current with slit height, after averaging over wavelength. The black curve shows data from a dark frame exposure on 21 February 2007 and the red curve shows data from 15 August 2009.

dark current rather than the detector.

In the bottom rows there is a region of reduced intensity around pixel 100. This dip is seen on all four wavelength quadrants of the bottom section of the detector. However, there is no equivalent intensity variation on the top section of the detector. This suggests that the dip in intensity is not due to the bias or dark current, but is a feature of the CCD pixels at this location on the detector.

The upward trend of the dark current with slit height, the sharp rise in dark current below pixel 30, and the dip in dark current around pixel 100 are evident in all the dark frame exposures sampled here. There has been a steady increase in the slope of the dark current with slit height over time. This can be seen by comparing the black and red curves in Figure 4.

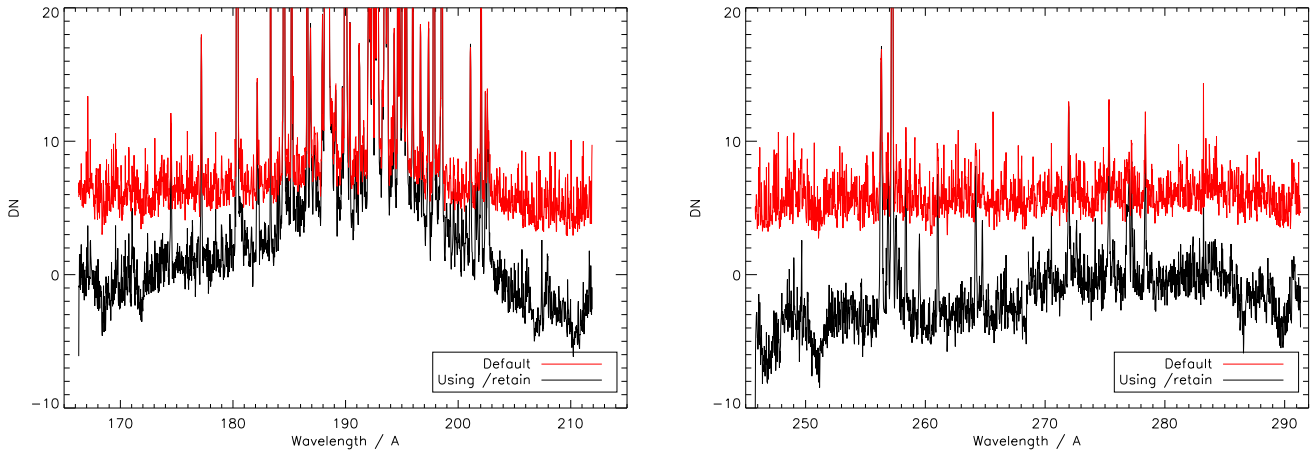

Figure 5: Spectra from an observation off the north pole. The short wavelength detector is shown on the left panel and the long wavelength detector is shown on the right panel. The red curves indicate the results from eis_prep with the default setting and the black curves indicate the results when the /retain keyword is set.

7 Impact on Data Analysis

The most important aspect of the `eis_prep` routine of which the user should be aware when analyzing data is the way in which it deals with pixels with negative counts after subtraction of the background. The default action is to flag any such pixels as missing. However, for full CCD observations of low emission regions (e.g., off disk, coronal holes, etc.) this can result in many pixels being incorrectly flagged as missing due to the background level being simplified to a constant over the entire detector. As can be seen in Figure 2, the background level is lowest at the wavelength extremes of the detectors. If the `/retain` keyword is set in `eis_prep` then pixels with zero or negative DN values will not be flagged as missing.

To show the importance of this on observation, we have selected a full CCD exposure at the north polar hole: file `eis_l0_20071116_072624.fits.gz`. Figure 5 shows the counts in DN from averaging all 7 pixels in the Solar-X direction and the top 50 pixels (of the full 512) in the Solar-Y direction: the area of the raster farthest from the limb and so lowest in emission. The black curve shows the average counts resulting from the default action of `eis_prep` (i.e., pixels with negative DN values are flagged as missing) while the red curve shows the counts when the `/retain` keyword is set (i.e., pixels with negative DN values are retained).

If DN is converted to intensity, the effects of fluctuation in the dark current are amplified where the effective area is low. This happens at the wavelength extremes of the detectors. Figure 6 shows the same observations as above, but with DN converted to intensity. The importance of using `/retain` is clearly demonstrated. One can also notice that the fluctuations in the background level (e.g., the troughs $\sim$ 247 and $\sim$ 251 Å) are amplified where the effective area of the detector is lowest.

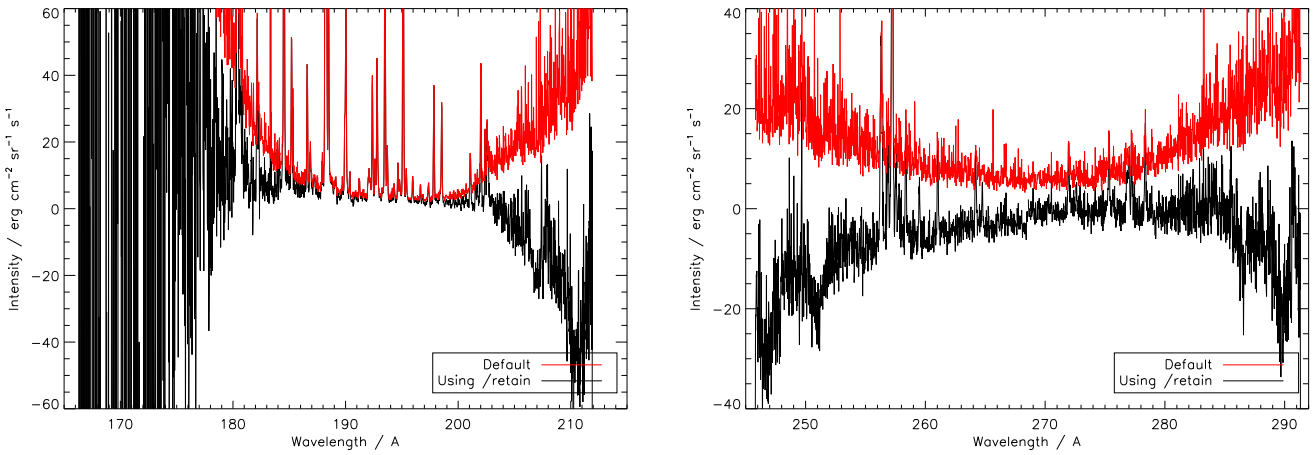

Figure 6: As Figure 5 but showing the spectra in units of intensity rather than DN.